Mutational Analysis of Fibrillarin and Its Mobility in Living Human Cells

Sabine Snaar, Karien Wiesmeijer, Aart G. Jochemsen, Hans J. Tanke, and Roeland W. Dirks

Department of Molecular Cell Biology, Sylvius Laboratories, Leiden University Medical Center, 2333 AL Leiden, The Netherlands

Abstract. Cajal bodies (CBs) are subnuclear organelles that contain components of a number of distinct pathways in RNA transcription and RNA processing. CBs have been linked to other subnuclear organelles such as nucleoli, but the reason for the presence of nucleolar proteins such as fibrillarin in CBs remains uncertain. Here, we use full-length fibrillarin and truncated fibrillarin mutants fused to green fluorescent protein (GFP) to demonstrate that specific structural domains of fibrillarin are required for correct intranuclear localization of fibrillarin to nucleoli and CBs. The second spacer domain and carboxy terminal alpha-helix domain in particular appear to target fibrillarin, respectively, to the nucleolar transcription centers and CBs. The presence of the RNP domain seems to be a prerequisite for correct targeting of fibrillarin. Time-lapse confocal microscopy of human cells that stably express fibrillarin-GFP shows that CBs fuse and split, albeit at low frequencies. Recovered fluorescence of fibrillarin-GFP in nucleoli and CBs after photobleaching indicates that it is highly mobile in both organelles (estimated diffusion constant $\sim$0.02 $\mu m^2\ s^{-1}$), and has a significantly larger mobile fraction in CBs than in nucleoli.

Key words: nucleolus • Cajal (coiled) body • confocal microscopy • fibrillarin • transfection

Introduction

The mammalian nucleus achieves a remarkably high level of compartmentalization despite the absence of separating membranes. This may occur either to perform its many functions in an organized fashion or as a result of these activities. A large variety of subnuclear organelles has been described, including nucleoli, Cajal bodies (CBs),[1] interchromatin granule clusters, Promyelocytic leukemia bodies, and gems (reviewed in Lamond and Earnshaw, 1998). The nucleolus is a highly dynamic structure that assembles at the ribosomal gene clusters and plays a role in many processes related to ribosome biogenesis. In addition, it is involved in the export of certain mRNAs and in processing of small RNA molecules (reviewed in Pederson, 1998). Electron microscopy reveals that the nucleolus consists of three different regions: fibrillar centers, dense fibrillar component, and granular component (Beven et al., 1996). Ribosomal RNA transcription apparently takes place within the dense fibrillar centers (Cmarko et al., 1999), possibly at the border with fibrillar centers (Dundr and Raska, 1993; Hozak, 1995). The nucleolus contains a large variety of proteins, including topoisomerase I, ribosomal protein S6, and Nopp140, and small nucleolar RNP components (snoRNP), such as U3 small nuclear (sn)RNA, NAP57, and fibrillarin (Matera, 1998).

CBs are highly conserved from plants to humans (de la Espina et al., 1982; Williams et al., 1983; Aris and Blobel, 1991; Beven et al., 1995), suggesting that they may fulfill essential cellular functions. CBs were first discovered as "nucleolar accessory bodies" by Ramón y Cajal in 1903, and have since then been shown to be structures of $\sim$0.2–1.5 μm containing the protein p80 coilin. This protein is present in a transcription-dependent concentration in CBs in combination with a diffuse nucleoplasmic pool (reviewed in Puvion-Dutilleul et al., 1991). P80 coilin has been demonstrated to target U7 snRNP to the CBs and to sites of histone pre-mRNA synthesis through association of a portion of the CBs with histone genes (Frey and Matera, 1995; Bellini and Gall, 1998). CBs have also been implicated in gene regulation as they associate with the gene loci of several U small nuclear RNA (snRNA) in a transcription-dependent manner (Smith et al., 1995; Gao et al., 1997; Schul et al., 1998; Frey et al., 1999).

Several aspects of a structural and/or functional connection between nucleoli and CBs have been elucidated. For example, expression of certain p80 coilin mutants results in loss of endogenous CBs, a dramatic disruption of nucleolar architecture and loss of RNA polymerase I activity (Bohmann et al., 1995a). CBs are often found adjacent to or within nucleoli in some cell types (Malatesta et al., 1994; Ochs et al., 1994) and these organelles share a number of

Address correspondence to Dr. R.W. Dirks, Department of Molecular Cell Biology, Laboratory for Cytochemistry and Cytometry, Sylvius Laboratories, Leiden University Medical Center, Wassenaarseweg 72, 2333 AL Leiden, The Netherlands. Tel.: 31-71-5276026. Fax: 31-71-5276180. E-mail: r.w.dirks@lumc.nl

[1]*Abbreviations used in this paper:* CB, Cajal body; D_{eff}, effective diffusion constant; GAR, glycine and arginine–rich; GFP, green fluorescent protein; TC, transcription center.

components including NAP57, Nopp140, and fibrillarin that may form a link between nucleoli and CBs. NAP57 and its yeast ortholog Cbf5p are both members of the box H/ACA snoRNPs and function in pseudouridylation of ribosomal RNA (Ganot et al., 1997; Lafontaine et al., 1998). Nopp140 interacts with the largest subunit of RNA polymerase I in vivo and functions in the transcription of rRNA genes (Chen et al., 1999). In addition, Nopp140 moves between nucleolus and cytoplasm, and between nucleolus and CBs and interacts directly with p80 coilin (Isaac et al., 1998). The function of fibrillarin in the CB is far from clear, but it may contribute to the molecular link between nucleoli and CBs in a manner similar to Nopp140.

Fibrillarin is highly conserved in sequence, structure, and function in eukaryotes (Schimmang et al., 1989; Henriquez et al., 1990; Lapeyre et al., 1990; Aris and Blobel, 1991; Jansen et al., 1991; Girard et al., 1993; Turley et al., 1993; Cappai et al., 1994; David et al., 1997). Fibrillarin, named Nop1p in yeast, is an essential component of box C/D snoRNPs (Tyc and Steitz, 1989; Aris and Blobel, 1991; Baserga et al., 1991) that function in site-specific 2′-*O*-methylation of pre-rRNA (Kiss-Laszlo et al., 1996; Tycowski et al., 1996; Dunbar and Baserga, 1998). Fibrillarin is directly involved in many posttranscriptional processes including pre-rRNA processing, pre-rRNA methylation, and ribosome assembly (Tollervey et al., 1993). Human fibrillarin consists of 321 amino acids and is predicted to have a molecular mass of 36 kD and three structural domains (Aris and Blobel, 1991). 80 NH_2-terminal amino acids comprise a glycine and arginine–rich (GAR) domain (Aris and Blobel, 1991) that is also present in fibrillarin of yeast and *Xenopus*, but not in *Tetrahymena* fibrillarin (David et al., 1997) and in a fibrillarin homologue of *Methanococcus jannaschii* (Wang et al., 2000). A central region of ~90 amino acids resembles an RNA-binding domain present in various snRNP proteins. The COOH terminus contains a small domain that may form alpha helices (Aris and Blobel, 1991). The crystal structure of a fibrillarin homologue from the hyperthermophile *Methanococcus jannaschii* shows a homodimerization domain in the NH_2-terminal region and a methyltransferase-like domain in the COOH-terminal region (Wang et al., 2000).

Since fibrillarin is present in both nucleoli and CBs, we sought to identify signal sequences that target these organelles. To this end, we constructed a number of truncated fibrillarin mutants, which were expressed as fusion proteins with green fluorescent protein (GFP) as an in vivo marker for protein localization. The distribution patterns of these fusion proteins in human cells indicate that separate domains target fibrillarin to nucleolar transcription centers and to CBs. In particular, the COOH-terminal alpha (α) domain appears to target fibrillarin to CBs, while the second spacer domain seems to target fibrillarin to nucleolar transcription centers, but this occurs only in the presence of the RNP domain. We also show that fibrillarin is highly mobile in both nucleoli and CBs.

Materials and Methods

Plasmid Constructs

Cloning was performed according to standard techniques (Sambrook et al., 1989). Full-length fibrillarin cDNA was amplified from total RNA of U-2 OS cells by standard reverse transcription (RT)–PCR procedures using specific primers containing an XbaI site. Enzymes used in this reaction were M-MLV RT (Life Technologies) and Pwo polymerase (Roche Diagnostics GmbH). The COOH terminus of fibrillarin cDNA was fused in frame to the GFP coding sequence by inserting it into the XbaI site of pGFP alpha (cycle III) (Crameri et al., 1996), which also contained a neomycin resistance gene. NH_2- and COOH-terminal deletion mutants of fibrillarin were generated by PCR from cDNA in an identical fashion. Internal mutants were constructed with primers spanning the junction between the remaining domains. All constructs were confirmed by sequencing.

Cell Lines, Cell Culture and Transfections Assays

Human osteosarcoma (U-2 OS) cells and HeLa cells are standard American Type Culture Collection cell lines. Cells were grown on sterile uncoated microscope glass slides in Dulbecco's Modified Eagle medium without phenol red containing 4.5 mg/ml glucose and 110 μg/ml sodium pyruvate, supplemented with 10% fetal calf serum, 0.03% glutamine, and 1000 U/ml penicillin/streptomycin (all from Life Technologies). Cells were cultured at 37°C in a 5% CO_2 atmosphere. Protein synthesis was inhibited by incubating the cells in medium containing 50 μg/ml cycloheximide (Sigma-Aldrich) for 4–6 h. Transient transfections of U-2 OS and HeLa cells were performed at ~60% confluence using DOTAP under conditions recommended by the manufacturer (Roche Diagnostics GmbH). Cells were analyzed by fluorescence microscopy 4–48 h after transfection. Distribution patterns of full-length or truncated fibrillarin-GFP were analyzed in 50–100 cells in at least two separate experiments. Plasmid DNA used in transfections was purified from bacterial cultures using maxiprep columns (QIAGEN). Transfected U-2 OS cells were grown in the presence of 400 μg/ml G418 (Promega) to obtain stable transfectants, and fibrillarin-GFP localization patterns were analyzed in ~30 stable clones by fluorescence microscopy. The FibGFP cell line was established from a representative clone.

Fixation and Immunofluorescence

Cells grown on glass slides were washed in PBS and fixed for 15 min with 3.7% wt/vol paraformaldehyde in CSK buffer (5 mM Pipes, pH 6.8, 50 mM NaCl, 150 mM sucrose, 1.5 mM $MgCl_2$, 1 mM EDTA) at room temperature. Cells were permeabilized before standard indirect immunofluorescence (Carmo-Fonseca et al., 1992) with 0.5% Triton X-100 (Sigma-Aldrich) in CSK buffer for 5 min at room temperature. The following antibodies were used: fibrillarin monoclonal antibody 72B9 (dilution 1:2), p80 coilin monoclonal antibody 5P10 (dilution 1:200), GFP monoclonal antibody 3E6 (dilution 1:100) (Quantum Biotechnologies Inc.), goat anti–mouse Cascade Blue (dilution 1:50), and goat anti–mouse Alexa 594 (dilution 1:500) (both from Molecular Probes, Inc.). U3 snRNA was detected by hybridization with a complementary 2′-*O*-methyl-RNA oligomer directly labeled with TAMRA. Fluorescence microscopy was carried out with a DM epifluorescence microscope, equipped with appropriate filter sets and a cooled CCD camera, or with a TCS confocal scanning laser microscope (Leica) using excitation wavelengths of 488 and 567 nm. Images were composed in Adobe Photoshop.

RNA Isolation and Northern Blotting

Northern blot analysis was performed according to standard methods (Sambrook et al., 1989). Total RNA was isolated from U-2 OS and fibrillarin-GFP cells by Trizol Reagent (Life Technologies). PolyA+ RNA was isolated from total RNA by the Poly ATtract mRNA isolation system (Promega) according to the protocol provided by the manufacturers. Specific probes for either fibrillarin or GFP RNA were generated by standard PCR methods from fibrillarin-GFP plasmid and labeled by random priming method with α-^{32}P-CTP.

Analysis of GFP Localization Patterns in Living Cells

Analysis of fibrillarin-GFP in living cells was carried out on cells grown on glass bottom petri dishes (MatTek Corp.) in the presence of Hepes-buffered RPMI 1640 without phenol red containing 2.0 mg/ml glucose, 5% fetal calf serum, 0.03% glutamine, and 1,000 U/ml penicillin/streptomycin. All reagents were obtained from Life Technologies. Dishes were placed in a temperature-controlled ring (Harvard Apparatus Inc.) on the stage of an Axiovert 135 TV inverted microscope (Carl Zeiss, Inc.). Images were acquired with a Xillix Microimager charge-coupled device camera, using a 40×, 1.3 NA oil immersion lens, which was maintained at 37°C by a controlled lens heater (Bioptechs). In addition, the system included motor-

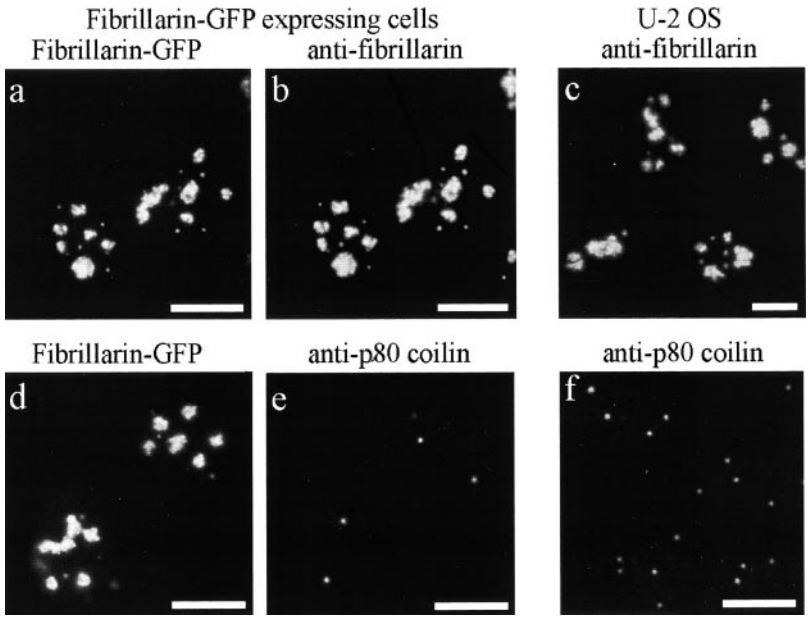

Figure 1. Control experiments validated the use of fibrillarin-GFP as a marker for fibrillarin localization. U-2 OS cells were transfected with fibrillarin-GFP, fixed, and subjected to indirect immunofluorescence staining. Scale bars indicate 10 μm. (a and d) Fibrillarin-GFP localized to Cajal bodies and in a nonuniform manner to nucleoli. (b) Localization of fibrillarin antigen in fibrillarin-GFP–expressing cells showed complete colocalization of fibrillarin-GFP with fibrillarin antigen. (c) Detection of endogenous fibrillarin in untransfected U-2 OS cells showed a distribution pattern similar to that of fibrillarin-GFP. (e and f) Localization of p80 coilin antigen was compared in cells expressing fibrillarin-GFP (e) and in untransfected U-2 OS cells (f).

ized shutters. Images were processed using ColourProc. Image stacks of cells were recorded with a TCS confocal microscope equipped with a temperature ring and controlled lens heater to maintain a temperature of 37°C. Image stacks were collected using a 100× NA 1.4 PL APO lens, and analyzed with accompanying software.

Fluorescence Recovery after Photobleaching

FRAP experiments were performed on a TCS confocal scanning laser microscope. Cells expressing fibrillarin-GFP were grown as for living cell analysis. Specific parts of the nucleus were bleached by laser beam parking for up to 5 s (White and Stelzer, 1999). Photobleaching removed <5% of total fluorescence. Image stacks of bleached and control cells in the same visual field were collected before and at a number of time points after bleaching, requiring ~30 s per stack. Corresponding differential interference contrast images were also recorded. Quantitative analysis of amount of fluorescence in bleached regions relative to unbleached regions was performed with TCS software and Excel. Estimation of the effective diffusion coefficients (D_{eff}) was carried out as described in Endow and Piston (1998) and Yguerabide et al. (1982).

Results

Fibrillarin-GFP Is Targeted to CBs and to Transcription Centers within Nucleoli

The localization and dynamic behavior of fibrillarin in living cells was studied by transient transfection of human U-2 OS and HeLa cells with a plasmid that codes for fibrillarin fused to GFP. Distribution patterns of fibrillarin-GFP were recorded by fluorescence microscopy at several times after 4–48 h. These images showed that fibrillarin-GFP was present at each of the time points both in nucleoli and in CBs immunofluorescently stained for p80 coilin (Fig. 1). Control experiments demonstrated that expression of fibrillarin-GFP did not alter the structure of nucleoli and CBs and that fibrillarin-GFP and endogenous fibrillarin had similar localization patterns in U-2 OS and

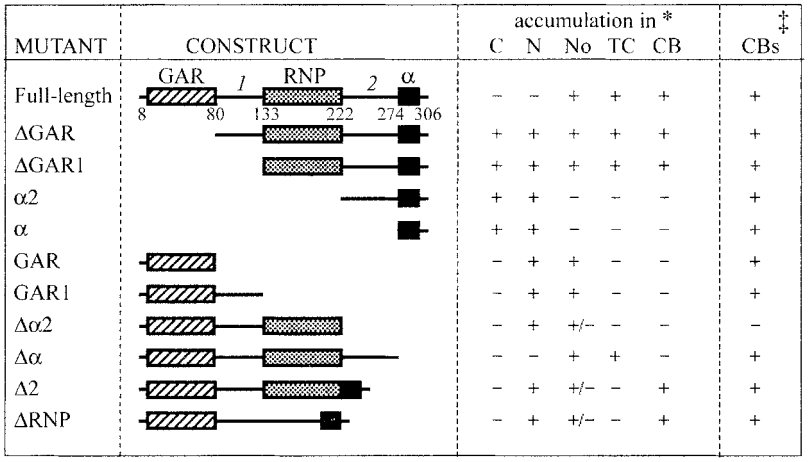

Figure 2. Schematic overview of mutant fibrillarin-GFP fusion constructs, showing the predicted domains in the secondary protein structure (Aris and Blobel, 1991). Each of the constructs was fused to GFP at its carboxy terminus. U-2 OS cells were transiently transfected with these constructs, and the localization of truncated fibrillarin-GFP was analyzed after ~24–30 h. *GAR,* glycine arginine rich domain; *RNP*, putative ribonucleotide binding domain; α, putative α-helical domain. 1 and 2 designate, respectively, the first and second spacer connecting these domains. Bar, 10 μm. *Detection of mutant fibrillarin-GFP in distinct subcellular compartments is indicated as: C, cytoplasm; N, nucleoplasm; No, nucleolus; TC, nucleolar transcription centers; and CB, Cajal bodies. Detection of fusion protein in most cells is indicated as (+), detection in ~50% of the cells as (+/−), or in almost none of the cells as (−). ‡Cajal bodies are present in cells expressing mutant fibrillarin-GFP, as detected by p80 coilin antibody 5P10. The presence of p80 coilin in Cajal bodies is indicated as (+), while the presence of p80 coilin in numerous small foci throughout the nucleoplasm was labeled as (−).

Table I. Fibrillarin-GFP Expression Does Not Affect the Average Number of CBs per Cell

	Number of CBs per cell		
	Average	SD	*n*
U-2 OS	2.9	1.3	159
Transient expression fibrillarin-GFP	3.4	1.4	100
Stable expression fibrillarin-GFP	3.3	1.3	215
(FibGFP cells)	3.3	1.3	215
Δα-GFP (transient)	2.7	1.3	100

Cajal bodies were detected with p80 coilin antibody 5P10 in untransfected and transfected U-2 OS cells. *n*, number of cells in which the number of Cajal bodies per cell was counted. Average numbers of Cajal bodies per cell and standard deviations were calculated from these data.

FibGFP cells (Fig. 1). Both endogenous fibrillarin and fibrillarin-GFP showed nonuniform staining of nucleoli with higher intensities in regions corresponding to transcription centers (TCs), as indicated by bromouridine incorporation (results not shown). Furthermore, both fibrillarin-GFP and endogenous fibrillarin showed perichromosomal localization in metaphase cells (results not shown) (Jimenez-Garcia et al., 1989; Yasuda and Maul, 1990), and fibrillarin-GFP expression did not alter the average numbers of CBs present in these cells (Table I). We used this system to examine which parts of the fibrillarin protein were required to target fibrillarin to nucleolar TCs and to CBs by transient expression of truncated fibrillarin-GFP fusion proteins. The deleted regions were predicted from the secondary structure of fibrillarin and involve the three structural domains in combination with two intervening spacers (Aris and Blobel, 1991) as shown in Fig. 2. Each of the constructs was transfected to U-2 OS cells, and its localization pattern was analyzed 24–30 h after transfection. Distribution patterns of each fibrillarin-GFP fusion protein were found to be identical in fixed and living cells (results not shown).

Specific Targeting of Fibrillarin to CBs Requires the COOH-Terminal α Domain

Truncated fibrillarin mutant Δα-GFP lacking the predicted COOH-terminal α-domain was not present in CBs (Fig. 3, d–f), but localized to nucleolar TCs. The average number of CBs detected by p80 coilin staining in these cells was indistinguishable from that in full-length fibrillarin-GFP expressing cells (Table I). Transfection of mutant α-GFP (consisting of only the α-domain fused to GFP) revealed a diffuse distribution pattern throughout the cell (Fig. 3, g–i) similar to the localization of the GFP vector alone (results not shown). These results suggested that the α-domain was required, but not sufficient, for targeting of fibrillarin to CBs.

Deletion of Both Second Spacer and α Domains Results in Relocation of Nuclear Proteins

Transfection of Δα2-GFP, lacking both α and second spacer domains, to U-2 OS cells resulted in two predominant GFP expression patterns. In the first, Δα2-GFP accumulated in numerous small foci in the nucleoplasm, but nucleoli remained unstained (Fig. 3, j–l). In the second pattern, transfected cells showed this punctuate nucleoplasmic distribution together with a uniform staining of the nucleoli (Fig. 4 a). Additional observations suggested that Δα2-GFP expression altered certain aspects of nuclear organization and functioning. First, cell viability was

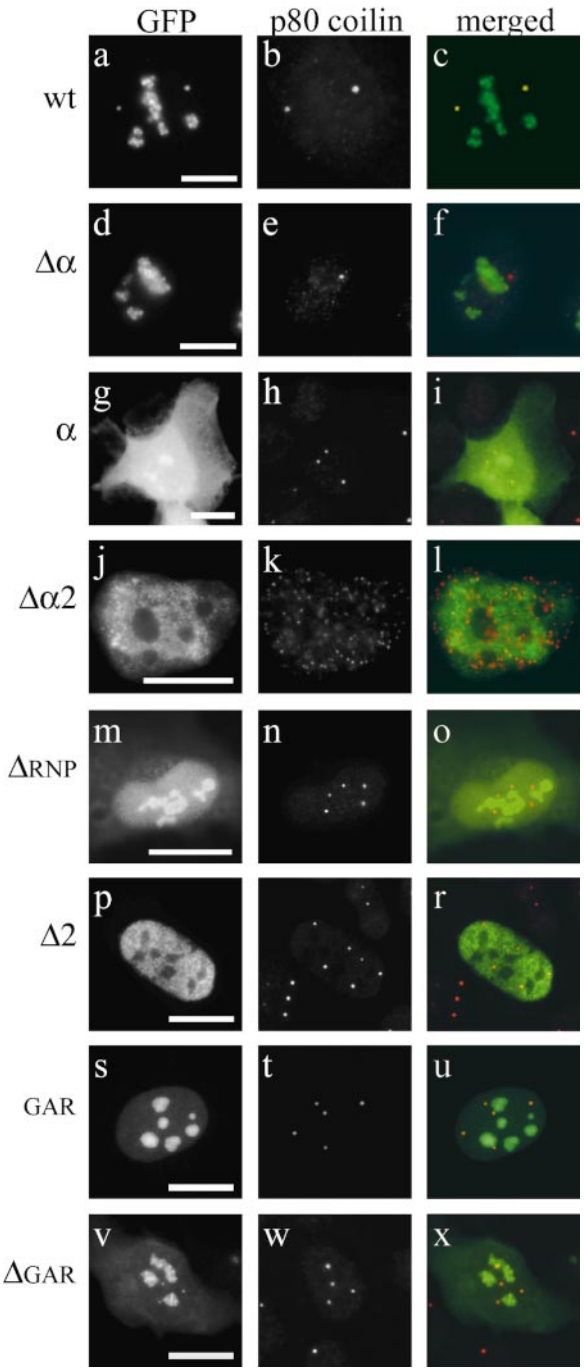

Figure 3. Distribution patterns of full-length and truncated fibrillarin fused to GFP. U-2 OS cells were transiently transfected with each of the constructs, and the localization of truncated fibrillarin-GFP was analyzed after ~24–30 h. The identity of the mutant concerned was indicated to the left of the images. Bars, 10 μm. (Left) The (mutant) fibrillarin-GFP distribution; (middle) localization of p80 coilin in the same cell as detected by monoclonal antibody 5P10. (Right) Merged images of (mutant) fibrillarin-GFP distribution (green) and p80 coilin (red). (a–c) Full-length fibrillarin-GFP is present both in nucleolar TCs and in Cajal bodies. (d–x) Distribution patterns of mutant fibrillarin-GFP constructs. These are discussed in detail in the text.

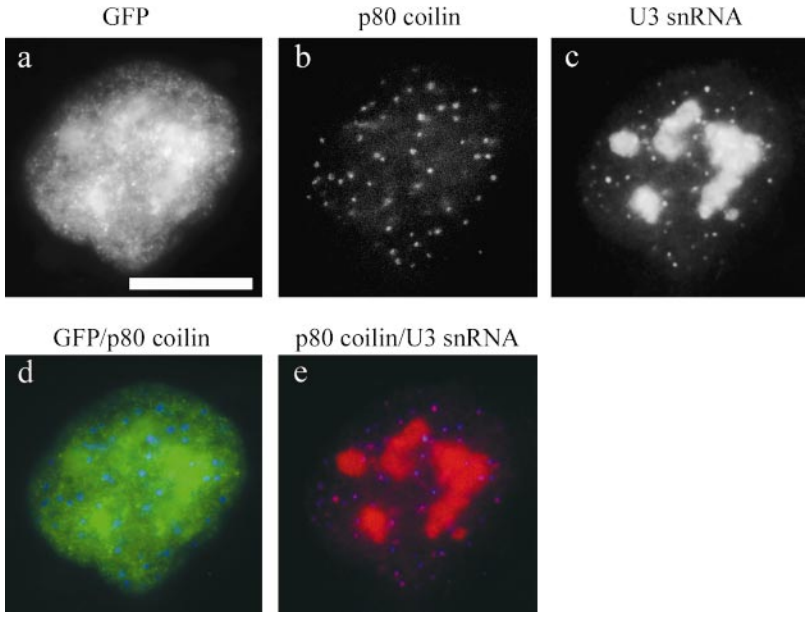

Figure 4. Expression of mutant Δα2-GFP results in redistribution of p80 coilin and U3 snRNA to the same small foci distributed throughout the nucleus. Cells were transiently transfected with Δα2-GFP, and U3 snRNA sequences were detected in combination with p80 coilin staining. Bar, 10 μm. (a) Δα2-GFP is present in a large number of nuclear foci, and is diffuse in nucleoli. (b) p80 coilin immunofluorescently detected by monoclonal antibody 5P10 is found in hundreds of small dots dispersed throughout the nucleoplasm. Each of these foci has a low fluorescent intensity relative to that of normal Cajal bodies. (c) Detection of U3 snRNA by hybridization with a specific 2′-*O*-methyl RNA oligonucleotide directly labeled with TAMRA. U3 snRNA is present in nucleoli and in a large number of nuclear foci. (d) Merged image of Δα2-GFP (green) and p80 coilin (blue). (e) Merged image of p80 coilin (blue) and U3 snRNA (red). Note the colocalization of p80 coilin and U3 snRNA factors in the small nuclear foci.

reduced, cell morphology deteriorated, and stable transfection was not possible. Second, p80 coilin was not present in CBs in most (76%; $n = 100$) of the cells, but was distributed to numerous small foci throughout the nucleoplasm (Figs. 3 k and 4 b). U3 RNAs colocalized exactly with p80 coilin in these small foci, suggesting that CBs were fragmented (Fig. 4, a–e). Furthermore, snRNP components of the splicing machinery were diffusely distributed in the nucleus, whereas they accumulate in speckles in normal U-2 OS cells (results not shown). Taken together, these results pointed to a dominant negative effect of Δα2-GFP expression on functioning or organization of endogenous fibrillarin that perturbs nuclear organization.

The Second Spacer Domain Targets Fibrillarin to TCs

Comparison of the localization patterns of the mutants Δα-GFP and Δα2-GFP suggested that the second spacer domain targeted fibrillarin to nucleolar TCs. To test this, we specifically deleted the second spacer domain in mutant Δ2-GFP. Its expression resulted in aberrant distribution patterns similar to those described for Δα2-GFP. In contrast to Δα2-GFP–expressing cells, cells expressing Δ2-GFP contained p80 coilin in CBs and in a weak nucleoplasmic pool in most cells (80%; $n = 100$) (Fig. 3, p–r). Thus, the relocation of nuclear factors like p80 coilin and U3 snRNA observed in Δα2-GFP–expressing cells did not occur in Δ2-GFP–expressing cells. α2-GFP was distributed throughout the entire cell (results not shown), as was α-GFP. This indicated that the presence of the second spacer domain was required but not sufficient for correct targeting of fibrillarin to nucleolar TCs.

The RNP Domain Is Required for Fibrillarin Targeting to Nucleolar TCs and CBs

Expression of mutant, lacking only the RNP domain, resulted in a diffuse staining of both nucleoplasm and nucleoli (Fig. 3, m–o). Nuclear organization appeared to be normal, as p80 coilin was present in CBs in the majority of these cells. However, ΔRNP-GFP did not localize to CBs. The presence of the RNP domain therefore appeared to be required, but not sufficient, for correct fibrillarin targeting.

The GAR Domain of Fibrillarin Contains a Nucleolar Localization Signal

U-2 OS cells were transfected with GAR-GFP to determine the function of the GAR domain in fibrillarin targeting since the GAR domain of RNA helicase II/Gu contains a nucleolar localization signal (Ou et al., 1999). GAR-GFP–expressing cells displayed an exclusively nuclear localization with diffuse staining of nucleoli and nucleoplasm (Fig. 3, s–u). Nucleolar staining in these cells was uniform and TCs and CBs were not discernible. The complementary mutant ΔGAR-GFP localized exactly as full-length fibrillarin-GFP in combination with a diffuse staining of both nucleoplasm and cytoplasm (Fig. 3, v–x). Taken together, these results suggested that the GAR domain contained a nucleolar localization signal that was not required to target fibrillarin to nucleolar TCs or CBs, but appeared to increase the efficiency of fibrillarin targeting. GAR1-GFP and ΔGAR1-GFP expression patterns were identical to those of GAR-GFP and ΔGAR-GFP, respectively. This showed that the first spacer domain did not have any observable effect on fibrillarin targeting (results not shown).

Dynamic Behavior of CBs in Living Human Cells: Observation of Fusion and Splitting Events

We studied the dynamic behavior of fibrillarin in living human cells using a stable U-2 OS cell line, FibGFP, expressing fibrillarin-GFP. Fibrillarin-GFP in FibGFP cells acted identical to fibrillarin-GFP expressed in transiently transfected cells, and thus colocalized with endogenous fibrillarin. FibGFP cells and U-2 OS cells also contained similar numbers of CBs (Table I). Furthermore, Northern blotting of polyA$^+$ RNA showed that messenger RNA expression levels of fibrillarin-GFP and endogenous fibrillarin were similar (results not shown). This indicated that expression of fibrillarin-GFP did not affect the expression level of endogenous fibrillarin. Therefore, we concluded that FibGFP cells provided a suitable model to examine fibrillarin mo-

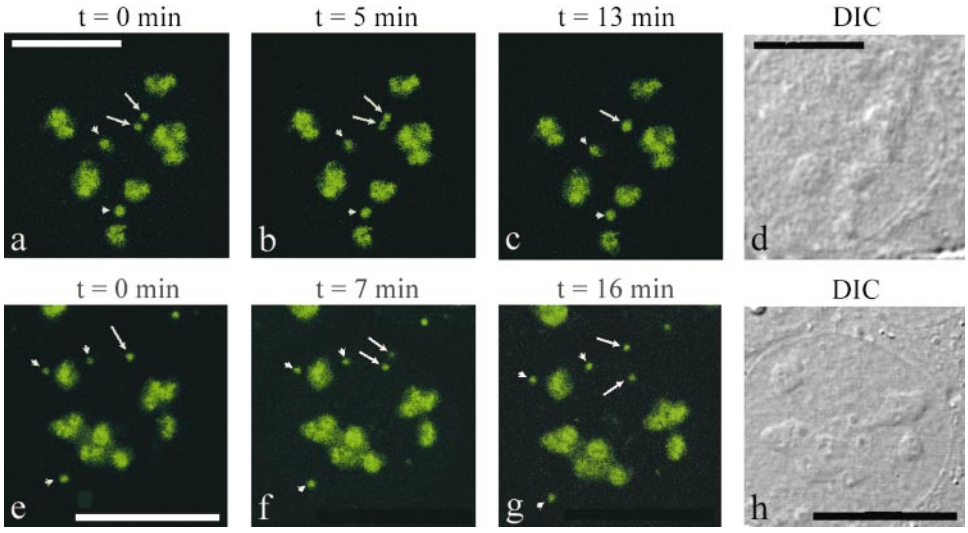

Figure 5. Cajal bodies in FibGFP cells are can fuse or split. The intranuclear position of Cajal bodies was followed for ~1 h by time-lapse confocal laser scanning microscopy in ~120 cells. Collection of image stacks through cells permitted three-dimensional reconstruction of the nucleus in order to ascertain that Cajal bodies occupied the same focal plane. Most Cajal bodies remained stationary during this time (arrowheads). Bars, 10 μm. (a–c) Confocal images of a fusion event (arrows). Two Cajal bodies moved towards each other, merged, and formed one large CB. (d) Corresponding differential interference contrast image. (e–g) Confocal images of a splitting Cajal body (arrows). One Cajal body splits into two independent Cajal bodies that subsequently move away from each other. (h) Corresponding differential interference contrast image.

bility in living cells. To determine whether CBs exhibit dynamic behavior in human cells, we followed the intranuclear positions of CBs in living FibGFP cells by time lapse CSLM for ~1 h. To reconstruct a three-dimensional representation of intranuclear CB positions, image stacks of each cell were collected, taking ~30 s per stack. This enabled us to ascertain that the CBs actually fused (or split), instead of merely passing over or below each other in dif-

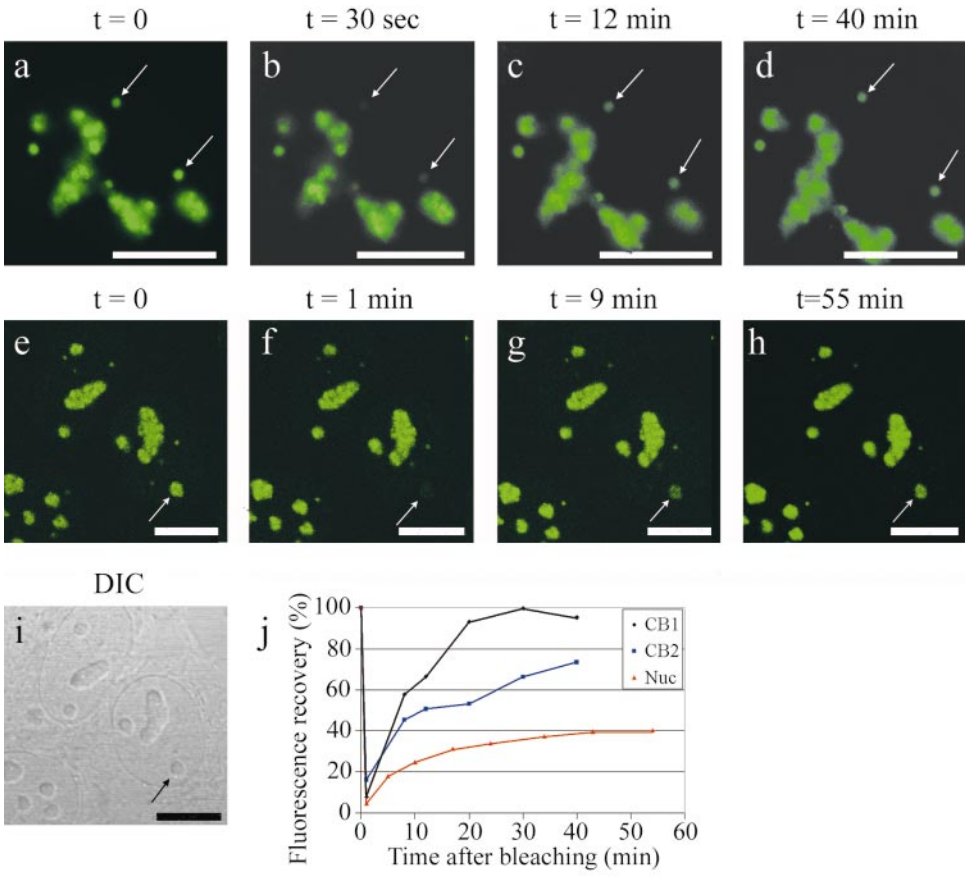

Figure 6. Example of a FRAP experiment. FibGFP cells were seeded on glass-bottom petri dishes and selected regions of the cell were photobleached by laser beam parking for up to 5 s. Images were collected on a TCS NT confocal scanning laser microscope (Leica). Bars, 10 μm. (a–d) Selection of time points demonstrating the bleaching and fluorescence recovery in two CBs (arrows). Image stacks were recorded before bleaching (a), immediately after bleaching (b), and at 12 min (c) and 40 min (d) after photobleaching. (e–i) Selection of time points showing FRAP of a nucleolus (arrow). Image stacks of this cell and control cells are shown before bleaching (e), immediately after bleaching (f), and 9 min (g) and 55 min (h) after bleaching. (i) Corresponding differential interference contrast image. (j) Quantitative analysis of FRAP of nucleoli (e–h) and Cajal bodies (a–d). Recovered fluorescence over time was quantified relative to an unbleached cellular compartment with TCS NT software and Excel.

ferent focal planes. The intranuclear positions of CBs in a large majority of cells (~98%) did not change significantly in this time. A major change in CB position was observed in the remaining 2% of the cells (2 of 120 cells), including movement of two CBs towards each other, followed by fusion to form one large CB (Fig. 5, a–d), and splitting of one CB into two independent CBs (Fig. 5, e–h).

Fibrillarin-GFP Is Highly Mobile in both CBs and Nucleoli

The relative mobility of fibrillarin-GFP molecules through nucleoli and CBs was assessed by FRAP measurements of fibrillarin-GFP in these subnuclear organelles. Confocal laser scanning microscopy image stacks of bleached and unbleached cells in the same visual field were recorded before and after bleaching. The amount of fluorescence in the three-dimensional region of interest at each time point was compared with the fluorescence intensity of an unbleached region in the same visual field. Photobleaching was irreversible (reviewed in White and Stelzer, 1999; Phair and Misteli, 2000) and did not affect cell viability, as FRAP experiments performed in the presence of propidium iodide showed that this compound remained excluded from the nucleus even after repeated exposure of the cell to photobleaching. The effective diffusion coefficients of fibrillarin-GFP determined from FRAP data were similar for nucleoli ($n = 17$) and CBs ($n = 8$) (Table II and Fig. 6). This indicated that movement of fibrillarin-GFP into CBs and nucleoli occurred at approximately the same rate. However, the mobile fraction of fibrillarin-GFP was significantly smaller in nucleoli (53 ± 4%) than in CBs (83 ± 11%; $P < 0.05$). Inhibition of protein synthesis did not change the D_{eff} or the mobile fraction, indicating that de novo protein synthesis was not required for recovery of fluorescence. FRAP analysis of a selection of truncated fibrillarin mutants suggested that the mobility of GAR-GFP was much higher than that of full-length fibrillarin and resembled the mobility of GFP itself. We were unable to estimate accurate D_{eff} values, since recovery in these cases was extremely fast compared with the time intervals required to collect images (typically 30 s). In contrast, ΔGAR-GFP showed a D_{eff} similar to that of full-length fibrillarin (Table II).

Table II. Estimated D_{eff} and Mobile Fractions of Fibrillarin-GFP in Nucleoli and in CBs

	Mobile fraction	SD	D_{eff}	*n*
	%	%	$\mu m^2\ s^{-1}$	
Fibrillarin-GFP in CBs (full-length)	83	11	0.02	17
Fibrillarin-GFP in nucleoli (full-length)	53	4	0.02	8
ΔGAR-GFP in CBs	90	ND	0.03	2

Cajal bodies or nucleoli in U-2 OS cells expressing full-length or truncated fibrillarin-GFP were photobleached by laser beam parking for up to 5 s. Image stacks were recorded by a time-lapse confocal scanning laser microscope to quantify fluorescence recovery relative to the fluorescent intensity of an unbleached object in the same visual field. Quantification was carried out by TCS NT software and Excel. D_{eff} was estimated as described in Endow and Piston (1998) and Yguerabide et al. (1982). *n*, number of independent bleaching experiments.

Discussion

The nucleolar functions of fibrillarin are well established and include pre-rRNA processing, pre-rRNA methylation, and ribosome assembly (Tollervey et al., 1993). Several models have been proposed to explain the presence of fibrillarin in CBs. The first model suggests that CBs originate from nucleoli, and fibrillarin may therefore be present in CBs as a structural constituent (Matera, 1999). The second model suggests that maturation processes or association with other nucleolar proteins occur during transit of newly synthesized fibrillarin through CBs. In an analogous manner, newly assembled snRNPs associate with CBs before they are transported to their final nuclear destinations, the interchromatin granule clusters and perichromatin fibrils, resulting in a maturation pathway for nuclear snRNPs through the CB (Sleeman and Lamond, 1999; Carvalho et al., 1999). Protein complexes required for transcription of all three polymerases also preassemble within CBs in *Xenopus laevis* before these unitary particles are transported to the sites of their activity (Gall et al., 1999). A third model suggests that fibrillarin performs one or more specific functions in CBs, perhaps in parallel with its nucleolar functions. Posttranscriptional processing of both rRNA and snRNA results in similar base and sugar modifications, such as 2′-*O*-methylation. This suggests that also the same or related enzymes may carry out these functions (Sleeman et al., 1998). As a fibrillarin homologue in *Methanococcus jannaschii* has been shown to contain a methylase fold (Wang et al., 2000), this enzymatic activity of fibrillarin may also be required in CBs. Here, we assess how the results of our study fit with the predictions generated by these models.

Fibrillarin-GFP Localization to CBs and Nucleoli Does Not Involve a Large Temporal Lag Phase

Transient expression of fibrillarin-GFP in U-2 OS cells shows that targeting of fibrillarin to nucleoli and CBs may occur simultaneously or with a short temporal lag phase of <4 h. Fibrillarin-GFP expression is not sufficient at shorter time points, and formation of the GFP fluorophore includes a rate-limiting step lasting several hours (Heim et al., 1994), thereby preventing the discrimination of distinct localization patterns. Nopp140 does not appear to chaperone fibrillarin to CBs, since Nopp140 only becomes visible in CBs ~12 h after its appearance in nucleoli (Isaac et al., 1998). The dynamics of fibrillarin localization also seem different than those of snRNPs, and a number of snoRNAs, which transit slowly through CBs (Gall et al., 1999; Natarayan et al., 1999; Sleeman and Lamond, 1999), thereby arguing against the second model. Fibrillarin may instead transit rapidly through CBs before transport to nucleoli occurs, as is suggested for the nucleolar protein NO38 (B23) (Peculis and Gall, 1992; Gall et al., 1999). However, the presence of Δα-GFP in nucleolar TCs but not in CBs suggests that fibrillarin can reach these organelles by separate pathways. This observation provides support for the third model, but is inconsistent with the first model.

The α, Second Spacer, and RNP Domains Are Required for Intranuclear Targeting of Fibrillarin

Complex signals appear to direct fibrillarin to the nucleus and to its intranuclear destinations. This is also the case for a number of other nucleolar proteins including p80 coilin (Bohmann et al., 1995b), nucleolin (Ginisty et al., 1999), and U2B″ (Boudonck et al., 1999). The deletion study demonstrates that fibrillarin requires the RNP, second

spacer, and α domains (amino acids 133–321) for correct localization. The second spacer domain and the α domain target fibrillarin, respectively, to nucleolar TCs and CBs, but this occurs only in the presence of the RNP domain. The second spacer domain also seems to be required for localization of p80 coilin to CBs. The region corresponding to the α domain in a *Methanococcus jannaschii* fibrillarin homologue contains an alpha helix followed by two beta strands that are part of a methyltransferase-like domain, which may be involved in enzymatic functioning of fibrillarin (Wang et al., 2000). A similar domain has been identified in yeast Nop1p (Niewmierzycka and Clarke, 1999). The mechanism that the α domain employs to target fibrillarin to CBs remains unknown. The transport of fibrillarin to CBs may result from its presence in complexes with certain snRNPs or proteins. Fibrillarin is generally complexed to box C/D U snoRNPs (Tollervey et al., 1993) and a direct interaction between unspecified regions of fibrillarin and U16 box C/D snoRNA has been reported (Fatica et al., 2000). This is supported by our observation that correct localization of fibrillarin does not occur in the absence of the RNP domain, which is most likely to interact with these factors. The observation that fibrillarin contains a specific signal in its amino acid sequence to target it to CBs also implies that the presence of fibrillarin in CBs may be necessary for other reasons than being a structural remnant due to the nucleolar origin of CBs.

Fibrillarin targeting to nucleolar TCs seems to require the second spacer domain, which may well be required for functional activity of fibrillarin as the nucleolar TC is thought to represent the site where fibrillarin performs its enzymatic activities (Dundr and Raska, 1993; Tollervey et al., 1993; Hozak, 1995; Beven et al., 1996; Lazdins et al., 1997; Cmarko et al., 1999). Point mutations in this region of yeast fibrillarin (Nop1p) cause defects in rRNA assembly and cleavage, thereby supporting its functional role (Tollervey et al., 1993). Expression of Δα2-GFP appears to have a detrimental effect on nuclear organization or functioning even in the presence of endogenous fibrillarin. Similar dominant negative effects have been shown for mutants of other proteins, such as p80 coilin (Bohmann et al., 1995a) and Nopp140 (Isaac et al., 1998). Again, this demonstrates the vital importance of the second spacer and α domains in targeting and possibly also in functioning of fibrillarin.

The GAR and First Spacer Domains Do Not Have Distinct Functions in Fibrillarin Targeting

The NH_2-terminal GAR domain of fibrillarin appears to contain a nucleolar localization signal, as does the GAR domain of RNA helicase II/Gu (Ou et al., 1999). Nucleolar targeting of the GAR domain may also occur through interactions with other ribosomal proteins, as has been shown for nucleolin (Bouvet et al., 1998). The GAR domain has recently been reported as necessary and sufficient for targeting of AtFbr1, a fibrillarin homologue in Arabidopsis, to nucleoli (Pih et al., 2000). However, in this study, no distinction was made between uniform and nonuniform staining of nucleoli. The GAR domain of human fibrillarin apparently increases the efficiency of fibrillarin targeting to nucleoli, but is neither sufficient nor required for targeting of fibrillarin. It is not conserved in prokaryotic fibrillarin (David et al., 1997; Wang et al., 2000), and point mutations with detrimental effects on the functioning of Nop1p in yeast have not been identified in this region (Tollervey et al., 1993). This suggests that the GAR domain is not required for enzymatic functioning of fibrillarin. The first spacer domain, which does not have any observable effect on fibrillarin localization, corresponds to a novel NH_2-terminal fold in *Methanococcus jannaschii* fibrillarin that acts as a homodimerization domain in the crystal (Wang et al., 2000). This implies that even though the first spacer domain may function as a dimerization domain in eukaryotes, it is not required for specific targeting of fibrillarin.

Cajal Bodies as Dynamic Compartments in Mammalian Cells

The intranuclear positions of CBs in most cells stably expressing full-length fibrillarin do not change within 1 h, but CBs in ~2% of the cells do show movement. Analysis of confocal image stacks demonstrates clearly that CBs can fuse or split. These observations are consistent with data reported for CB dynamics in Arabidopsis root cells (Boudonck et al., 1999). Similar events are also observed in other mammalian cell types expressing GFP-coilin, although at a higher frequency (Platani, Swedlow, and Lamond, manuscript in preparation). The functional significance of these events remains unknown. CBs may act as transport shuttles between nucleoplasm and nucleoli (Boudonck et al., 1999), but the low frequency of CB movement suggests that additional transport mechanisms are likely to exist.

Fibrillarin-GFP Is Highly Mobile, and Its Mobile Fraction Is Larger in CBs than in Nucleoli

It is unlikely that the only function of fibrillarin in CBs is that of a structural component, since binding of fibrillarin-GFP to nucleoli and CBs in FRAP experiments is extensive and rapid. This implies that fibrillarin molecules are only present at CBs and nucleoli for a short time. The estimated effective diffusion constant of 0.02 $\mu m^2\ s^{-1}$ for fibrillarin in nucleoli and CBs is similar to the value that Phair and Misteli (2000) have reported. The mobile fraction of fibrillarin-GFP molecules is significantly larger in CBs than in nucleoli (84% vs. 53%; $P < 0.05$). The functional significance of this difference is yet unknown, but mobile and immobile fractions of fibrillarin-GFP may represent molecules with different cellular functions, such as enzymatic versus structural roles. Alternatively, different amounts of fibrillarin may be stored at these sites. The high mobile fraction of fibrillarin-GFP in CBs would then indicate that relatively few of these molecules serve structural roles. Return of fluorescent fibrillarin-GFP to CBs also continues in the absence of newly formed fibrillarin. This argues against the second model, which explains the presence of fibrillarin in CBs as transit of newly formed fibrillarin through CBs in a maturation or assembly pathway. Several observations suggest that trafficking of fibrillarin-GFP may occur in any direction between nucleoplasm, CBs, and nucleoli, and is most likely governed by a passive mechanism (Phair and Misteli, 2000). First, bleaching of large nucleolar structures does not result in decreased fluorescence intensity in CBs. Second, unbleached CBs are not required for recovery of fluorescence in

bleached CBs or nucleoli. Thus, in agreement with conclusions reached by Matera (1998), CBs do not appear to function as storage sites for nucleolar factors. A variant of the second model proposes that recycled fibrillarin molecules transit through the CB to be preassembled into protein complexes associated with polymerase I transcription (Gall et al., 1999). The continuous binding of fibrillarin to CBs may therefore reflect an ongoing flow of proteins and snoRNA components first heading for preassembly in CBs, and then to their sites of biological activity. However, the presence of Δα-GFP in nucleolar TCs, but not in CBs, demonstrates that this process is not absolutely required for targeting of fibrillarin-GFP to nucleoli.

FRAP experiments with complementary mutants, namely GAR-GFP and ΔGAR-GFP, suggest that their different localization patterns are reflected by differences in dynamic behavior. GAR-GFP shows diffuse nuclear staining and uniform nucleolar staining, and probably does not interact with the same nuclear factors as fibrillarin. FRAP data of this mutant suggest that its fluorescence recovery is at least one order of magnitude faster than that of full-length fibrillarin. It is instead similar to the speed of fluorescence recovery of GFP alone. This suggests that GAR-GFP diffuses freely throughout the nucleus. In contrast, the distribution patterns of full-length fibrillarin and ΔGAR-GFP are similar with the addition of a dispersed staining of the nucleoplasm. This may reflect the involvement of these proteins in interactions with the same nuclear factors. FRAP data again support this, as ΔGAR-GFP displays kinetics similar to those of full-length fibrillarin. In conclusion, though the function of fibrillarin in CBs remains to be elucidated, it is appealing to speculate that fibrillarin is involved in similar enzymatic reactions in CBs as in nucleoli (Sleeman et al., 1998). To clarify this, the identification of nuclear factors interacting with the structural domains of fibrillarin will be needed.

We thank A.I. Lamond for critical reading of the manuscript and for generously providing p80 coilin antibody (mAb 5P10). We thank K.M. Pollard for kindly providing fibrillarin antibody (mAb 72B9) and Eurogentec (Seraing, Belgium) for supplying the 2′-*O*-methyl RNA-TAMRA. We also thank J.W. Gray for critical reading of the manuscript.

Submitted: 3 May 2000
Revised: 10 August 2000
Accepted: 15 September 2000

References

Aris, J.P., and G. Blobel. 1991. cDNA cloning and sequencing of human fibrillarin, a conserved nucleolar protein recognized by autoimmune antisera. *Proc. Natl. Acad. Sci. USA*. 88:931–935.

Baserga, S.J., X.D. Yang, and J.A. Steitz. 1991. An intact box C sequence in the U3 snRNA is required for binding of fibrillarin, the protein common to the major family of nucleolar snRNPs. *EMBO (Eur. Mol. Biol. Organ.) J.* 10:2645–2651.

Bellini, M., and J.G. Gall. 1998. Coilin can form a complex with the U7 small nuclear ribonucleoprotein. *Mol. Biol. Cell.* 9:2987–3001.

Beven, A.F., G.G. Simpson, J.W.S. Brown, and P.J. Shaw. 1995. The organization of spliceosomal components in the nuclei of higher plants. *J. Cell Sci.* 108:509–518.

Beven, A.F., R. Lee, M. Razaz, D.J. Leader, J.W.S. Brown, and P.J. Shaw. 1996. The organization of ribosomal RNA processing correlates with the distribution of nucleolar snRNAs. *J. Cell Sci.* 109:1241–1251.

Bohmann, K., J.A. Ferreira, and A.I. Lamond. 1995a. Mutational analysis of p80 coilin indicates a functional interaction between coiled bodies and the nucleolus. *J. Cell Biol.* 131:817–831.

Bohmann, K., J. Ferreira, N. Santama, K. Weis, and A.I. Lamond. 1995b. Molecular analysis of the coiled body. *J. Cell Sci.* 19:107–113.

Boudonck, K., L. Dolan, and P.J. Shaw. 1999. The movement of coiled bodies visualized in living plant cells by the green fluorescent protein. *Mol. Biol. Cell.* 10:2297–2307.

Bouvet, P., J.-J. Diaz, K. Kindbeiter, J.-J. Madjar, and F. Amalric. 1998. Nucleolin interacts with several ribosomal proteins through its RGG domain. *J. Biol. Chem.* 273:19025–19029.

Cappai, R., A.H. Osborn, and E. Handman. 1994. Cloning and sequence of a *Leishmania major* homologue to the fibrillarin gene. *Mol. Biochem. Parasitol*. 64:353–355.

Carmo-Fonseca, M., R. Pepperkok, M.T. Carvalho, and A.I. Lamond. 1992. Transcription-dependent colocalization of the U1, U2, U4/U6, and U5 snRNPs in coiled bodies. *J. Cell Biol.* 117:1–14.

Carvalho, T., F. Almeida, A. Calapez, M. Lafarga, M.T. Berciano, and M. Carmo-Fonseca. 1999. The spinal muscular atrophy disease gene product, SMN: a link between snRNP biogenesis and the Cajal (coiled) body. *J. Cell Biol.* 147:715–728.

Chen, H.K., C.-Y. Pai, J.Y. Huang, and N.H. Yeh. 1999. Human Nopp140, which interacts with RNA polymerase I: implications for rRNA gene transcription and nucleolar structural organization. *Mol. Cell. Biol.* 19:8536–8546.

Cmarko, D., P.J. Verschure, T.E. Martin, M.E. Dhamus, S. Krause, X.-D. Fu, R. van Driel, and S. Fakan. 1999. Ultrastructural analysis of transcription and splicing in the cell nucleus after bromo-UTP microinjection. *Mol. Biol. Cell.* 10:211–223.

Crameri, A., E.A. Whitehorn, E. Tate, and W.P.C. Stemmer. 1996. Improved green fluorescent protein by molecular evolution using DNA shuffling. *Nat. Biotechnol*. 14:315–319.

David, E., J.B. McNeil, V. Basile, and R.E. Pearlman. 1997. An unusual fibrillarin gene and protein: structure and functional implications. *Mol. Biol. Cell*. 8:1051–1061.

Dunbar, D.A., and S.J. Baserga. 1998. The U14 snoRNA is required for 2′-*O*-methylation of the pre-18S rRNA in *Xenopus* oocytes. *RNA (NY)*. 4:195–204.

Dundr, M., and I. Raska. 1993. Nonisotopic ultrastructural mapping of transcription sites within the nucleolus. *Exp. Cell Res.* 208:275–281.

Endow, S.A., and D.W. Piston. 1998. Methods and protocols. *In* GFP Green Fluorescent Protein. Properties, Applications, and Protocols. M. Chalfie, and S. Kain, editors. Wiley-Liss, New York. 271–369.

de la Espina, S.M., M.A. Sanchez-Pina, and M.C. Risueno. 1982. Localization of acid phosphatase activity, phosphate ions, and inorganic cations in plant nuclear coiled bodies. *Cell Biol. Int. Rep.* 6:601–607.

Fatica, A., S. Galardi, F. Altieri, and I. Bozzoni. 2000. Fibrillarin binds directly and specifically to U16 box C/D snoRNA. *RNA (NY)*. 6:88–95.

Frey, M.R., and A.G. Matera. 1995. Coiled bodies contain U7 small nuclear RNA and associate with specific DNA sequences in interphase human cells. *Proc. Natl. Acad. Sci. USA*. 92:5915–5919.

Frey, M.R., A.D. Bailey, A.M. Weiner, and A.G. Matera. 1999. Association of snRNA genes with coiled bodies is mediated by nascent snRNA transcripts. *Curr. Biol.* 9:126–135.

Gall, J.G., M. Bellini, Z. Wu, and C. Murphy. 1999. Assembly of the nuclear transcription and processing machinery: Cajal bodies (coiled bodies) and transcriptosomes. *Mol. Biol. Cell.* 10:4385–4402.

Gao, L., M.R. Frey, and A.G. Matera. 1997. Human genes encoding U3 snRNA associate with coiled bodies in interphase cells and are clustered on chromosome 17p11.2 in a complex inverted repeat structure. *Nucleic Acids Res.* 25:4740–4747.

Ganot, P., M. Caizergues-Ferrer, and T. Kiss. 1997. The family of box ACA small nucleolar RNAs is defined by an evolutionarily conserved secondary structure and ubiquitous sequence elements essential for RNA accumulation. *Genes Dev*. 11:941–956.

Ginisty, H., H. Sicard, B. Roger, and P. Bouvet. 1999. Structure and functions of nucleolin. *J. Cell Sci.* 112:761–772.

Girard, J.P., J. Feliu, M. Caizergues-Ferrer, and B. Lapeyre. 1993. Study of multiple fibrillarin mRNAs reveals that 3′ end formation in *Schizosaccharomyces pombe* is sensitive to cold shock. *Nucleic Acids Res*. 21:1881–1887.

Heim, R., D.C. Prasher, and R.Y. Tsien. 1994. Wavelength mutations and posttranslational autooxidation of green fluorescent protein. *Proc. Natl. Acad. Sci. USA*. 91:12501–12504.

Henriquez, R., G. Blobel, and J.P. Aris. 1990. Isolation and sequencing of NOP1.A yeast gene encoding a nucleolar protein homologous to a human autoantigen. *J. Biol. Chem.* 265:2209–2215.

Hozak, P. 1995. Catching RNA polymerase I in flagranti: ribosomal genes are transcribed in the dense fibrillar component of the nucleolus. *Exp. Cell Res.* 216:285–289.

Isaac, C., Y. Yang, and U.T. Meier. 1998. Nopp140 functions as a molecular link between the nucleolus and the coiled bodies. *J. Cell Biol.* 142:319–329.

Jansen, R.P., E.C. Hurt, H. Kern., H. Lehtonen, M. Carmo-Fonseca, B. Lapeyre, and D. Tollervey. 1991. Evolutionary conservation of the human nucleolar protein fibrillarin and its functional expression in yeast. *J. Cell Biol.* 113:715–729.

Jimenez-Garcia, L.F., L.I. Rothblum, H. Busch, and R.L. Ochs. 1989. Nucleologenesis: use of non-isotopic in situ hybridization and immunocytochemistry to compare the localization of rDNA and nucleolar proteins during mitosis. *Biol. Cell.* 65:239–246.

Kiss-Laszlo, Z., Y. Henry, J.P. Bachellerie, M. Caizergues-Ferrer, and T. Kiss. 1996. Site-specific ribose methylation of preribosomal RNA: a novel function for small nucleolar RNAs. *Cell.* 85:1077–1088.

Lafontaine, D.L.J., C. Bousquet-Antonelli, Y. Henri, M. Caizergues-Ferrer, and D. Tollervey. 1998. The box H+ ACA snoRNAs carry Cbf5b, the putative rRNA pseudouridine synthase. *Genes Dev*. 12:527–537.

Lamond, A.I., and W.C. Earnshaw. 1998. Structure and function in the nucleus. *Science.* 280:547–553.

Lapeyre, B., P. Mariotinni, D. Mathieu, P. Ferrer, F. Amaldi, F. Amalric, and M. Caizergues-Ferrer. 1990. Molecular cloning of *Xenopus* fibrillarin, a conserved U3 small nuclear ribonucleoprotein recognized by antisera from humans with autoimmune disease. *Mol. Cell. Biol.* 10:430–434.

Lazdins, I.B., M. Delannoy, and B. Sollner-Webb. 1997. Analysis of nucleolar transcription and processing domains and pre-rRNA movements by in situ hybridization. *Chromosoma.* 105:481–495.

Malatesta, M., C. Zancanaro, T.E. Martin, E.K. Chan, F. Amalric, R. Luhrmann, P. Vogel, and S. Fakan. 1994. Cytochemical and immunocytochemical characterization of nuclear bodies during hibernation. *Eur. J. Cell Biol.* 65:82–95.

Matera, A.G. 1998. Of coiled bodies, gems, and salmon. *J. Cell. Biochem.* 70: 181–192.

Matera, A.G. 1999. Nuclear bodies: multifaceted subdomains of the interchromatin space. *Trends Cell Biol.* 9:302–309.

Natarayan, A., W. Speckmann, R. Terns, and M.P. Terns. 1999. Role of the box C/D motif in localization of small nucleolar RNAs to coiled bodies and nucleoli. *Mol. Biol. Cell.* 10:2131–2147.

Niewmierzycka, A., and S. Clarke. 1999. S-adenosylmethionine–dependent methylation in *Saccharomyces cerevisiae*. *J. Biol. Chem.* 274:814–824.

Ochs, R.L., T.W. Stein, and E.M. Tan. 1994. Coiled bodies in the nucleolus of breast cancer cells. *J. Cell Sci.* 107:385–399.

Ou, Y., M.J. Fritzler, B.C. Valdez, and J.B. Rattner. 1999. Mapping and characterization of the functional domains of the nucleolar protein RNA helicase II/Gu. *Exp. Cell Res.* 247:389–398.

Peculis, B.A., and J.G. Gall. 1992. Localization of the nucleolar protein NO38 in amphibian oocytes. *J. Cell Biol.* 116:1–14.

Pederson, T. 1998. The plurifunctional nucleolus. *Nucleic Acids Res.* 26:3871–3876.

Phair, R.D., and T. Misteli. 2000. High mobility of proteins in the mammalian cell nucleus. *Nature.* 404:604–609.

Pih, K.T., M.J. Yi, Y.S. Liang, B.J. Shin, M.J. Cho, I. Hwang, and D. Son. 2000. Molecular cloning and targeting of a fibrillarin homolog from Arabidopsis. *Plant Physiol.* 123:51–58.

Puvion-Dutilleul, F., S. Mazan, M. Nicoloso, M.E. Christensen, and J.P. Bachellerie. 1991. Localization of U3 RNA molecules in nucleoli of HeLa and mouse 3T3 cells by high resolution in situ hybridization. *Eur. J. Cell Biol.* 56:178–186.

Sambrook, J., E.F. Fritsch, and T. Maniatis. 1989. Molecular Cloning: A Laboratory Manual. Second edition. Cold Spring Harbor Laboratory Press, Cold Spring Harbor, NY.

Schimmang, T., D. Tollervey, H. Kern, R. Frank, and E.C. Hurt. 1989. A yeast nucleolar protein related to mammalian fibrillarin is associated with small nucleolar RNA and is essential for viability. *EMBO (Eur. Mol. Biol. Organ.) J.* 8:4015–4024.

Schul, W., R. van Driel, and L. de Jong. 1998. Coiled bodies and U2 snRNA genes adjacent to coiled bodies are enriched in factors required for snRNA transcription. *Mol. Biol. Cell.* 9:1025–1036.

Sleeman, J., C.E. Lyon, M. Platani, J.-P. Kreivi, and A.I. Lamond. 1998. Dynamic interactions between splicing snRNPs, coiled bodies, and nucleoli revealed using snRNP protein fusions to the green fluorescent protein. *Exp. Cell Res.* 243:290–304.

Sleeman, J.E., and A.I. Lamond. 1999. Newly assembled snRNPs associate with coiled bodies before speckles, suggesting a nuclear snRNP maturation pathway. *Curr. Biol.* 9:1065–1074.

Smith, K.P., K.C. Carter, C.V. Johnson, and J.B. Lawrence. 1995. U2 and U1 snRNA gene loci associate with coiled bodies. *J. Cell. Biochem.* 59:473–485.

Tollervey, D., H. Lehtonen, R. Jansen, H. Kern, and E.C. Hurt. 1993. Temperature-sensitive mutations demonstrate roles for yeast fibrillarin in pre-rRNA processing, pre-rRNA methylation, and ribosome assembly. *Cell.* 72:443–457.

Turley, S.J., E.M. Tan, and K.M. Pollard. 1993. Molecular cloning and sequence analysis of U3 snoRNA-associated mouse fibrillarin. *Biochim. Biophys. Acta.* 1216:119–122.

Tyc, K., and J.A. Steitz. 1989. U3, U8 and U13 comprise a new class of mammalian snRNPs localized in the cell nucleolus. *EMBO (Eur. Mol. Biol. Organ.) J.* 8:3113–3119.

Tycowski, K.T., C.M. Smith, M.D. Shu, and J.A. Steitz. 1996. A small nucleolar RNA requirement for site-specific ribose methylation of rRNA in *Xenopus*. *Proc. Natl. Acad. Sci. USA*. 93:14480–14485.

Wang, H., D. Boisvert, K.K. Kim, R. Kim, and S.-H. Kim. 2000. Crystal structure of a fibrillarin homologue from *Methanococcus jannaschii*, a hyperthermophile, at 1.6 Å resolution. *EMBO (Eur. Mol. Biol. Organ.) J.* 19:317–323.

White, J., and E. Stelzer. 1999. Photobleaching GFP reveals protein dynamics inside living cells. *Trends Cell Biol.* 9:61–65.

Williams, L.M., E.G. Jordan, and P.W. Barlow. 1983. The ultrastructure of nuclear bodies in interphase plant cell nuclei. *Protoplasma.* 118:99–103.

Yasuda, Y., and G.G. Maul. 1990. A nucleolar auto-antigen is part of a major chromosomal surface component. *Chromosoma.* 99:152–160.

Yguerabide, J., J.A. Schmidt, and E.E. Yguerabide. 1982. Lateral mobility in membranes as detected by fluorescence recovery after photobleaching. *Biophys. J.* 40:69–75.